DRIFT OF ICEBERGS AFFECTED BY WAVE ACTION

AZMY FOUAD ABOUL-AZM

DRIFT OF ICEBERGS AFFECTED BY WAVE ACTION

By

© Azmy Fouad Aboul-Azm, B.Sc.(Eng)

A Thesis submitted in partial fulfillment of the requirements for the degree of:

© Master of Engineering

Faculty of Engineering and Applied Science
Memorial University of Newfoundland
St. John's, Newfoundland, Canada

December 1982

ABSTRACT

The wave drift force acting on freely floating icebergs has been analysed. This wave drift force was included together with other environmental forces acting on an iceberg for drift modelling to predict its drift patterns.

The wave drift force was calculated using the wave diffraction theory and the singularity distribution method. By distributing singularities over the underwater surface of the iceberg, the velocity potential due to wave diffraction was computed using the Green's function method, and then added to the incoming wave velocity potential to form the total velocity potential. It was assumed that the potential due to the oscillatory motion of an iceberg was negligible. The wave drift force was derived by taking the time average of the second-order wave forces on the iceberg.

The computed wave drift force was then added to other environmental forces acting on the iceberg to form the differential equations of motion for translation in a horizontal plane. The iceberg trajectory can be found by solving the equations of motion numerically with the time step integration technique.

This study has shown that the wave drift force acting on an iceberg is significant and has the same order of magnitude as other environmental forces. Including the wave drift force in the drift model has improved the accuracy of predicted paths of icebergs. This was verified by comparing the observed and predicted trajectories of two icebergs with and without the wave drift effect.

ACKNOWLEDGEMENT

The author is grateful to Professor C.C. Hsiung for his enthusiastic supervision and encouragement throughout the duration of this work.

The valuable encouragement by Dr. G.R. Peters, Dean of Engineering and Applied Science, is also gratefully acknowledged.

TABLE OF CONTENTS

LIST OF TABLES

LIST OF FIGURES

NOMENCLATURE

x, y, z	=	Cartesian Co-ordinate System
Φ	=	Velocity Potential
ϕ	=	Velocity Potential function of space coordinates only.
ω	=	Oscilliation frequency
t	=	Time
i	=	$\sqrt{-1}$
ϕ_I	=	Incident velocity potential due to waves.
ϕ_D	=	Velocity potential due to wave diffraction.
h	=	Water depth in meters.
C	=	Complex function.
S	=	Body surface.
r & σ	=	Polar Co-ordinates.
g	=	Gravitational acceleration.
k	=	Wave Number.
β	=	Direction of propagation of incident wave with respect to x axis.
f	=	Source density function.
G	=	Green's function.
ξ, η, ζ	=	Co-ordinate of a point on the under water body surface.
R	=	$\left[(x-\xi)^2 + (y-\eta)^2 + (z-\zeta)^2\right]^{1/2}$
R'	=	$\left[(x-\xi)^2 + (y+2h+\eta)^2 + (z-\zeta)^2\right]^{1/2}$
r	=	$\left[(x-\xi)^2 + (z-\zeta)^2\right]^{1/2}$

P.V.	=	Cauchy principal value of the infinite integral.
ν	=	ω^2/g
μ	=	Dummy variable of integration.
J_o	=	Bessel function of the first kind of zero order.
J	=	Bessel function of the first kind.
Y_o	=	Bessel function of the second kind.
K_o	=	Modified Bessel function of the second kind of zero order.
μ_k	=	Real positive roots of the equation: $\mu_k \tan(\mu_k h) + \nu = 0$
R_1	=	$\left[r^2 + (y + \eta)^2\right]^{1/2}$
R_{2n}	=	$\left[r^2 + (y - 2nh - \eta)^2\right]^{1/2}$
R_{3n}	=	$\left[r^2 + (y + 2nh + \eta)^2\right]^{1/2}$
R_{4n}	=	$\left[r^2 + (y + 2nh - \eta)^2\right]^{1/2}$
R_{5n}	=	$\left[r^2 + (y - 2nh + \eta)^2\right]^{1/2}$
n	=	Outward unit normal vector on the surface S.
n_x, n_y, n_z	=	Components of the unit normal to the surface S, in the x, y, and z directions respectively.
N	=	Total number of facets over the immeresed surface of the iceberg.
F_{wd}	=	Wave drift force.
P	=	Pressure.
S_o	=	Wetted body surface below the still water level.
WL	=	Waterline curve of the body at $y = 0$

ε	=	Perturbation parameter with respect to hydrostatic pressure.
η	=	Wave elevation.
ρ	=	Density of sea water.
ϕ^1	=	Second order velocity potential.
F_1	=	First order wave force.
F_2	=	Second order wave force.
F	=	~~Total wave force.~~
T	=	Wave Period.
η_a	=	Wave amplitude.
L	=	Length of the projected waterline perpendicular to wave propagation direction.
m	=	Mass of the iceberg.
δm	=	Added mass coefficient.
$[m + \delta m]$	=	Virtual mass matrix.
$[C]$	=	Wave damping coefficient matrix.
$[K]$	=	Hydrostatic restoring coefficient matrix.
$\vec{F}_e$	=	Environmental forces vector.
$\vec{\xi}$	=	Displacement vector.
$\dot{\vec{\xi}}$	=	Velocity vector.
$\ddot{\vec{\xi}}$	=	Acceleartion Vector.
$\vec{v}$	=	(u, w), iceberg velocity.
$\vec{v}_a$	=	(u_a, w_a), wind velocity.
$\vec{v}_{cj}$	=	(u_{cj}, w_{cj}), water current velocity at jth layer of iceberg underwater.

$\vec{v}_g$	=	(u_g, w_g), geostrophic current velocity.
v_n	=	Magnitude of the normal component of velocity on the immersed surface of the iceberg.
C_a	=	Air drag coefficient.
ρ_a	=	Air density.
C_w	=	Water drag coefficient.
A_a	=	Projected area of iceberg profile above water, perpendicular to wind direction.
A_{wj}	=	Projected area of iceberg profile of jth layer of underwater portion, perpendicular to current direction.
γ	=	$2\Omega \sin \psi$, Coriolis parameter.
Ω	=	Angular velocity of earth.
ψ	=	Iceberg latitude.
j	=	1, 6, modes of motion (six degrees of freedom).
$\dot{\eta}_j$	=	Body velocity in the jth mode of motion.
ϕ_j	=	The contribution to velocity potential from the jth mode of motion.

CHAPTER I

INTRODUCTION

The recent discovery of hydrocarbons in the Grand Bank area near Newfoundland is good news for this energy-thirsty world, but there are many hazardous problems that will be encountered for any type of offshore operations. One of the problems is iceberg drift in the Grand Bank area, since the presence of icebergs has the potential to interrupt offshore activities. Furthermore, iceberg scouring may damage any facilities mounted on the ocean floor.

Analysis of iceberg response to different environmental conditions is important for studying its behaviour. In order to avoid an iceberg hazard, one has to predict iceberg path, which in turn depends on iceberg geometrical parameters and the environmental forces driving it. Environmental forces affecting iceberg drift pattern consist of current force, pressure gradient due to ocean surface slope, wind drag, water acceleration, Coriolis effect and wave drift effect.

The trajectory of iceberg drift can be predicted from mathematical models in a form of differential equations relating iceberg parameters and environmental forces affecting its motion. Mathematical models for predicting drift trajectories have been developed among others, by, Sodhi and Dempster [1], Napoleoni [2], Mountain [3], Sodhi and El-Tahan [4]. The environmental forces considered were consisted of Coriolis force, current force, wind force, and the force due to geostropic water current. However, the wave drift force has always been neglected.

In this thesis wave drift force has been presented and calculated using three dimensional singularity distribution method. The wave drift force has then been included together with other environmental forces to form an iceberg drift model. The model's differential equations of motion were solved by time-step integration techniques to produce predicted iceberg trajectory. Predicted trajectories based on the mathematical models both with and without wave effect have been calculated and compared with observed results from the field.

CHAPTER II

WAVE DRIFT FORCE

2.1 Wave Forces

Icebergs floating in the ocean are subjected to wave action which may be represented by two forces:

(a) First order wave force:

This force is linearly proportional to the wave amplitude, and it has the same frequencies as those of the encountered waves. It is periodic in nature with a zero mean for time average [5].

(b) Second order wave force:

This force is a time averaging and slowly varying force with frequencies below wave frequencies. Its magnitude is proportional to the square of the encountered wave amplitude [6].

The first order wave force is the so-called periodic wave exciting force. This force is responsible for the periodic motion of floating bodies (in six degrees of freedom) with frequencies similar to those of the waves, and is predominate in the analysis of wave loading on offshore structures.

However, it is the second order wave force which causes any freely floating body to drift away from its initial position. Thus the second order wave force, namely the wave drift force is also important in the mooring forces analysis for floating structures in waves. Only the wave drift force is of interest in this study.

2.2 Hydrodynamic Boundary Value Problem

Consider an iceberg floating freely in waves, with under water surface $S(x, y, z) = 0$, as shown in Figure 1, where:

Oxyz is a cartesian co-ordinate system.

O is the origin located on the waterplane, vertically above the center of gravity of iceberg.

xz-plane is parallel to the calm water surface.

y-axis is pointing upward.

Assuming that the fluid is homogenous, invicid, and incompressible with a finite depth of h; and that the flow is irrotational. A velocity potential Φ is introduced to describe the fluid motion. The total velocity potential Φ can be written as:

$$\Phi(x,y,z;t) = \text{Re}\ \{\phi(x,y,z)\ e^{-i\omega t}\} + \sum_{j=1}^{6} \phi_j\ \eta_j \qquad (2.1)$$

where:

ϕ = The velocity potential, which is a function of space co-ordinates only.

Re = The real part of a complex function.

$i = \sqrt{-1}$

ω = Oscillation frequency.

t = Time.

j = 1, 6, modes of motion (six degrees of freedom).

ϕ_j = The contribution to velocity potential from the jth mode of motion.

η_j = Body displacement in the jth mode of motion.

The velocity potential $\phi(x,y,z)$ can be conviently broken down into two parts:

1. Velocity potential due to incident wave $\phi_I(x,y,z)$.
2. Velocity potential due to wave diffraction $\phi_D(x,y,z)$.

It is assumed that the amplitude of the oscillatory motion of a very large floating body, like iceberg, is very small, and that the velocity potential due to body oscillation ϕ_j may be neglected without affecting the accuracy of calculation. Hence, the velocity potential components will only consist of the parts due to incident waves and diffraction waves; i.e.

$$\phi(x,y,z) = \phi_I(x,y,z) + \phi_D(x,y,z) \qquad (2.2)$$

The velocity potential must satisfy Laplace equation:

$$\frac{\partial^2\phi}{\partial x^2} + \frac{\partial^2\phi}{\partial y^2} + \frac{\partial^2\phi}{\partial z^2} = 0 \tag{2.3}$$

The solution of Laplace equation will be in the fluid domain surrounding the iceberg, and subjected to the boundary conditions. The fluid domain extends from the free surface ($y = 0$) to the ocean floor ($y = -h$), where h is the water depth, and from the iceberg under water surface S to infinity. The boundary conditions can be written as:

1. Free surface boundary conditions on $y = 0$.

$$-\omega^2\phi + g\frac{\partial\phi}{\partial y} = 0 \tag{2.4}$$

2. The bottom condition on $y = -h$.

$$\left.\frac{\partial\phi}{\partial y}\right|_{y=-h} = 0 \tag{2.5}$$

3. The radiation condition, in polar co-ordinate system.

$$\phi_D(r,\theta,y) \to C(\theta)r^{-1/2}\,\frac{\cosh k(h+y)}{\cosh kh}\,e^{ikr} \text{ as } r\to\infty \tag{2.6}$$

Where:

r & θ = polar co-ordinates

k = wave number, defined as $k = 2\pi/L$

r = $\left[x^2 + z^2\right]^{1/2}$

θ = $\tan^{-1}(z/x)$

C = unknown complex function with $C(\theta)r^{-1/2}$

4. Body boundary condition:

$$\frac{\partial \phi_D}{\partial n} = -\frac{\partial \phi_I}{\partial n} = v_n \quad \text{on surface S.} \qquad (2.7)$$

Where:

n = The outward unit normal vector to the iceberg surface S.

v_n = Magnitude of the normal component of velocity of the immersed surface of the body.

The boundaries of the fluid domain for the boundary value problem are shown in Figure 2.

2.3 Solution of the Boundary Value Problem

The solution of the boundary value problem, formulated in the previous section (Section 2.2), is the velocity potential $\phi(x,y,z)$. The velocity potential of the incident wave ϕ_I can be written, from the linear wave theory as:

$$\phi_I = \frac{g\eta_a}{2\omega} \frac{\cosh k(h+y)}{\cosh kh} e^{i(kx \cos \beta + kz \sin \beta)} \quad (2.8)$$

Where:

g = gravitational acceleration.

ω = wave frequency.

k = wave number, which is related to the frequency of the waves by the dispersion relationship:

$\omega^2/g = k \tanh(kh)$.

h = water depth.

β = direction of propagation of incident waves.

η_a = wave amplitude.

The velocity potential due to wave diffraction ϕ_D can be solved in terms of Green's function method. Based on Green's theorem, it is possible to show that ϕ_D can be written as:

$$\phi_D = \iint_S f(\xi,\eta,\zeta) G(x,y,z;\xi,\eta,\zeta)\, ds \quad (2.9)$$

Where:

f = unknown source density function.

ξ,η,ζ = co-ordinates of a surface point.

x,y,z = co-ordinates of a field point.

$G(x,y,z;\xi,\eta,\zeta)$ = Green's function.

The integration in equation (2.9) is over the wetted surface S of the iceberg.

The particular expression for Green's function G, appropriate to the boundary-value problem posed, is given by Wehausen and Laitone [8], and it may take one of the following forms:

1. Integral form:

$$G = \frac{1}{R} + \frac{1}{R'} + 2\ \mathrm{P.V.} \int_0^\infty \frac{(\mu+\nu)e^{-\mu h}\cosh[\mu(\eta+h)]\cosh[\mu(y+h)]}{\mu \sin h(\mu h) - \nu \cosh(\nu h)} J_o(\mu r)\, d\mu$$

$$+ i\, \frac{2\pi(k^2-\nu^2)\cosh[k(\eta+h)]\cosh[k(y+h)]}{k^2 h - \nu^2 h + \nu} J_o(kr) \qquad (2.10)$$

Where:

$R = \left[(x-\xi)^2 + (y-\eta)^2 + (z-\zeta^2)\right]^{1/2}$

$R' = \left[(x-\xi)^2 + (y+2h+\eta)^2 + (z-\zeta)^2\right]^{1/2}$

$r = \left[(x-\xi)^2 + (z-\zeta)^2\right]^{1/2}$

P.V. = Cauchy principal value of the infinite integral

$\nu = \omega^2/g = k \tanh(kh)$

μ = dummy variable of integration.

J_o = Bessel function of the first kind of order zero.

$i = \sqrt{-1}$

2. Summation form:

$$G = \frac{2\pi(\nu^2-k^2)}{k^2h-\nu^2h+\nu} \cosh[k(\eta+h)]\cosh[k(y+h)][Y_o(kr) - iJ_o(kr)]$$

$$+ 4\sum_{k=1}^{\infty} \frac{(\mu_k^2+\nu^2)}{\mu_k^2h+\nu^2h-\nu} \cos[\mu_k(y+h)]\cos[\mu_k(\eta+h)]\; K_o(\mu_k r) \tag{2.11}$$

Where:

Y_o = Bessel function of the second kind.

J = Bessel function of the first kind.

K_o = Modified Bessel function of the second kind of zero order.

μ_k = real positive roots of the equation $\mu_k \tan(\mu_k h)+\nu=0$.

3. Series form, after Garrison [10]:

$$G = \frac{1}{R} + \frac{1}{R_1} + \sum_{n=1}^{\infty}\left[\frac{1}{R_{2_n}} + \frac{1}{R_{3_n}} + \frac{1}{R_{4_n}} + \frac{1}{R_{5_n}}\right] \tag{2.12}$$

Where:

$R = \left[r^2 + (y-\eta)^2\right]^{1/2}$

$r = \left[(x-\xi)^2 + (z-\zeta)^2\right]^{1/2}$

$R_1 = \left[r^2 + (y+\eta)^2\right]^{1/2}$

$R_{2_n} = \left[r^2 + (y-2nh-\eta)^2\right]^{1/2}$

$R_{3_n} = \left[r^2 + (y+2nh+\eta)^2\right]^{1/2}$

$R_{4_n} = \left[r^2 + (y+2nh-\eta)^2\right]^{1/2}$

$R_{5_n} = \left[r^2 + (y-2nh+\eta)^2\right]^{1/2}$

The third form of Green's function (series form) is appropriate for the case where the period of the motion is very large, as might occur in the interaction of waves of large period with large body. This form of Green's function is more appropriate for the case of iceberg in waves, and it has been used for this study.

The source strength f in equation (2.9) are calculated to satisfy the kinematic boundary condition on the wetted surface S, so that the normal component of the fluid velocity is zero. This results in the following Fredholm integral equation of the second kind over the surface S:

$$-f(x,y,z) + \frac{1}{2\pi}\iint_S f(\xi,\eta,\zeta)\,\frac{\partial G}{\partial n}(x,y,z;\xi,\eta,\zeta)\,dS = 2v_n(x,y,z) \tag{2.13}$$

Where:

$\frac{\partial G}{\partial n}$ = the derivatives of the Green's function in the outward normal direction.

n = outward unit normal vector on the surface S.

The derivatives of the Green's function $\partial G/\partial n$ can be written as:

$$\frac{\partial G}{\partial n} = \frac{\partial G}{\partial x}n_x + \frac{\partial G}{\partial y}n_y + \frac{\partial G}{\partial z}n_z \tag{2.14}$$

Where: n_x, n_y, and n_z are components of the unit normal to the surface S, in the x, y and z directions respectively.

Equation (2.13) is to be satisfied at all points (x,y,z) over the wetted surface S of the iceberg.

Solution of the Fredholm integral equation of the second kind will give the source strength function f in equation (2.13). Once the function f is found, it is possible to obtain the diffraction velocity potential ϕ_D using the following relation:

$$\phi_D = \frac{1}{4\pi} \iint_S f(\xi,\eta,\zeta) G(x,y,z;\xi,\eta,\zeta) ds \qquad (2.15)$$

where the integration in this equation is over the wetted surface of the body.

2.4 Numerical Solution for Velocity Potential

Solution of the Fredholm integral equation of the second kind has been achieved by using numerical solution scheme. The average underwater surface S of the iceberg has been divided into a large number j of small facets each with area S_j, as shown in Figure 3. The centroids of the facets were taken as node points and their coordinates have been identified. The source strength function f, may then be represented as the distribution of source strengths f_j at each nodel point j over the surface S. The derivatives of Green's function with respect to unit normal vector, can also be calculated at each single nodal point j considering the rest of the surface nodal points k. This can be represented as α_{kj}, which is an element of a matrix of the size k by j and can be calculated from the following relation:

$$\alpha_{kj} = \frac{1}{2\pi} \iint_{\Delta S_j} \frac{\partial G}{\partial n} (x_k, y_k, z_k; \xi, \eta, \zeta)\, dS \qquad (2.16)$$

Similarly the derivatives of the incident wave velocity potential ϕ_I, can be calculated at each nodal point of the surface S, and represented as the vector v_{nj}. Fredholm equation (equation 2.13) can then be written in the matrix form as:

$$-f_j + \alpha_{kj}\, f_k = 2v_{nj} \quad k, j = 1, 2, \ldots, N \qquad (2.17)$$

or:

$$\left[f\right] = 2\left[\alpha - I\right]^{-1}\left[v_n\right] \qquad (2.18)$$

The matrix equation (2.18), has been solved numerically using the matrix inversion technique, which is usually used for solving sets of simultaneous linear equations. The solution of equation (2.18) is the source strength vector $[f]$, and can be substituted into equation (2.15) to obtain the wave diffraction velocity potential ϕ_D. Equation (2.15) will then take the matrix form:

$$\{\phi_D\} = \{\beta\}\left[f\right] \qquad (2.19)$$

In equation (2.19) the elements of the matrix $\{\beta\}$ have been obtained from the following relation:

$$\beta_{kj} = \frac{1}{4\pi} \iint_{\Delta S_j} G(x_k, y_k, z_k; \xi, \eta, \zeta) dS \tag{2.20}$$

From equation (2.19) the diffraction velocity potential at each nodal point j can be obtained. Substituting the co-ordinates of each facet centroid into equation (2.8), the incident velocity potential at the jth nodal point on the surface can then be written as:

$$\phi_j = \phi_{Ij} + \phi_{Dj} \tag{2.21}$$

2.5 Wave Drift Force

Assuming that the fluid is homogenous, invicid, incompressible and irrotational, the wave force acting on a floating body can be calculated from the potential theory. Wave force can be calculated by integrating the fluid pressure over the wetted surface of the body, and it can be expressed in vector form as:

$$F = -\iint_S p n dS = -\iint_{S_o} p n dS - \int_{WL} \left[\int_0^{\eta} p dy\right] n d\ell \tag{2.22}$$

Where:

S = instantaneous wetted surface of the body.

S_o = the wetted body surface below the still water level (y=0).

WL = the water line curve of the body at $y = 0$.

n = outer normal vector.

In equation (2.22) an area element dS of the intermittently wet portion of the surface has been expressed as $(dy.d\ell)$, since the body surface in the vicinity may be considered vertical. Since the pressure variation near the free surface is hydrostatic to the first order, the pressure integral in the second part of the right hand side of equation (2.22) can be written as:

$$\int_0^{\eta} p\,dy = \int_0^{\eta} \{\rho g(\eta - y) + 0\left[\varepsilon^3\right]\}\, dy = \varepsilon^2 \;(1/2\rho g \eta^2) + 0\left[\varepsilon^3\right] \tag{2.23}$$

Where:

ε = perturbation parameter with respect to hydrostatic.

η = wave elevation

ρ = density of water.

The pressure on the body surface, to the second order, can be written from Bernoulli's equation as:

$$p = \rho g y + \varepsilon\left[-\rho\frac{\partial\phi}{\partial t}\right] + \varepsilon^2\left[-\rho\frac{\partial\phi^1}{\partial t} - 1/2\,\rho\,|\nabla\phi|^2\right] + 0\;\left[\varepsilon^3\right] \tag{2.24}$$

Where:

ϕ = first order velocity potential.

ϕ^1 = second order velocity potential.

The total wave force acting on the body can be written as:

$$F = \varepsilon F_1 + \varepsilon^2 F_2 + O(\varepsilon^3) \tag{2.25}$$

Where:

F_1 = First order wave force.

F_2 = Second order wave force.

Substituting equation (2.23) and (2.24) into equation (2.22) and comparing the resulting terms with the terms in equation (2.25), the first and second order wave forces can be written as:

$$F_1 = \rho \iint_{S_o} \frac{\partial \phi}{\partial t} n dS \tag{2.26}$$

$$F_2 = \rho \iint_{S_o} \frac{\partial \phi}{\partial t} n dS + 1/2\rho \iint_{So} |\nabla\phi|^2 ndS - 1/2\rho \int_{WL} \eta^2 d\ell \tag{2.27}$$

Taking the time average of the total force, the first order wave force (equation 2.26) and the first term in equation (2.27) will vanish, and the wave drift force can then be written as:

$$F_{WD} = \frac{1}{T}\int_0^T dt \{1/2\rho \iint |\nabla\phi|^2 ndS - 1/2\rho g \int_{WL} \eta^2 d\ell\} \tag{2.28}$$

or:

$$F_{WD} = \frac{1}{T}\int_0^T dt \{1/2\rho \iint |\nabla\phi|^2 nds\} - \frac{1}{T}\int_0^T dt \{1/2\rho g \int_{WL} \eta^2 d\ell\} \tag{2.29}$$

The first integration in equation (2.29) can be found:

$$[\nabla\phi]^2 = (\frac{\partial\phi}{\partial x})^2 + (\frac{\partial\phi}{\partial y})^2 + (\frac{\partial\phi}{\partial z})^2 \tag{2.30}$$

and as $\phi = \phi_I + \phi_D$

$$(\frac{\partial\phi}{\partial x})^2 = (\frac{\partial\phi_I}{\partial x} + \frac{\partial\phi_D}{\partial x})^2$$

$$(\frac{\partial\phi}{\partial y})^2 = (\frac{\partial\phi_I}{\partial y} + \frac{\partial\phi_D}{\partial y})^2$$

$$(\frac{\partial\phi}{\partial z})^2 = (\frac{\partial\phi_I}{\partial z} + \frac{\partial\phi_D}{\partial z})^2 \tag{2.31}$$

In equation (2.31), the derivatives of incident wave potential can be written as:

$$\frac{\partial\phi_I}{\partial x} = \frac{g\eta_a\, k\, \cos\beta}{2\omega}\ \frac{\cosh k\,(h+y)}{\cosh kh}\ \sin\left[k(x\cos\beta + z\sin\beta)\right]$$

$$\frac{\partial\phi_I}{\partial y} = \frac{g\eta_a\, k}{2\omega}\ \frac{\sinh k\,(h+y)}{\cosh kh}\ \cos\left[k(x\cos\beta + z\sin\beta)\right]$$

$$\frac{\partial\phi_I}{\partial z} = \frac{g\eta_a\, k\, \sin\beta}{2\omega}\ \frac{\cosh k\,(h+y)}{\cosh kh}\ \sin\left[k(x\cos\beta + z\sin\beta)\right] \tag{2.32a}$$

Also, from equation (2.7):

$$v_n = -(\frac{\partial\phi_I}{\partial x} n_x + \frac{\partial\phi_I}{\partial y} n_y + \frac{\partial\phi_I}{\partial z} n_z) \tag{2.32b}$$

The derivatives of diffracted wave potential are:

$$\frac{\partial\phi_D}{\partial x} = \frac{1}{4\pi} \iint_S f\ \frac{\partial G}{\partial x}\,(x,y,z;\xi,\eta,\zeta)\ ds$$

$$\frac{\partial \phi_D}{\partial y} = \frac{1}{4\pi} \iint_S f \; \frac{\partial G}{\partial y} \; (x,y,z;\xi,\eta,\zeta) \; dS$$

$$\frac{\partial \phi_D}{\partial z} = \frac{1}{4\pi} \iint_S f \; \frac{\partial G}{\partial z} \; (x,y,z;\xi,\eta,\zeta) \; dS \tag{2.33}$$

In which, from equation (2.12).

$$\begin{aligned}
\frac{\partial G}{\partial x} = -\; (x-\xi) \; \{ & \left[(x-\xi)^2+(y-\eta)^2+(z-\zeta)^2\right]^{-3/2} \\
& + \left[(x-\xi)^2+(y+\eta)^2+(z-\zeta)^2\right]^{-3/2} \\
& + \left[(x-\xi)^2+(y-2nh-\eta)^2+(z-\zeta)^2\right]^{-3/2} \\
& + \left[(x-\xi)^2+(y+2nh+\eta)^2+(z-\zeta)^2\right]^{-3/2} \\
& + \left[(x-\xi)^2+(y+2nh-\eta)^2+(z-\zeta)^2\right]^{-3/2} \\
& + \left[(x-\xi)^2+(y-2nh+\eta)^2+(z-\zeta)^2\right]^{-3/2} \}
\end{aligned}$$

$$\begin{aligned}
\frac{\partial G}{\partial y} = & -\; (y-\eta) \; \left[(x-\xi)^2+(y-\eta)^2+(z-\zeta)^2\right]^{-3/2} \\
& - (y+\eta) \left[(x-\xi)^2+(y+\eta)^2+(z-\zeta)^2\right]^{-3/2} \\
& - (y-2nh-\eta) \left[(x-\xi)^2+(y-2nh-\eta)^2+(z-\zeta)^2\right]^{-3/2} \\
& - (y+2nh+\eta) \left[(x-\xi)^2+(y+2nh+\eta)^2+(z-\zeta)^2\right]^{-3/2} \\
& - (y+2nh-\eta) \left[(x-\xi)^2+(y+2nh-\eta)^2+(z-\zeta)^2\right]^{-3/2} \\
& - (y+2nh+\eta) \left[(x-\xi)^2+(y-2nh+\eta)^2+(z-\zeta)^2\right]^{-3/2}
\end{aligned}$$

$$\begin{aligned}
\frac{\partial G}{\partial y} = -\; (z-\zeta) \; \{ & \left[(x-\xi)^2+(y-\eta)^2+(z-\zeta)^2\right]^{-3/2} \\
& + \left[(x-\xi)^2+(y+\eta)^2+(z-\zeta)^2\right]^{-3/2}
\end{aligned}$$

$$+ \left[(x-\xi)^2+(y-2nh-\eta)^2+(z-\zeta)^2\right]^{-3/2}$$
$$+ \left[(x-\xi)^2+(y+2nh+\eta)^2+(z-\zeta)^2\right]^{-3/2}$$
$$+ \left[(x-\xi)^2+(y+2nh-\eta)^2+(z-\zeta)^2\right]^{-3/2}$$
$$+ \left[(x-\xi)^2+(y-2nh+\eta)^2+(z-\zeta)^2\right]^{-3/2} \qquad (2.34)$$

In the second integration of equation (2.29) the wave elevation can be obtained from the following relation:

$$\eta = \frac{1}{g}\frac{\partial\phi_I}{\partial t} = \frac{1}{g}\frac{\partial}{\partial t}\left[\phi_I(x,y,z)\, e^{-i\omega t}\right] \qquad (2.35)$$

or:

$$\eta = \frac{g\eta_a}{2}\frac{\cosh k(h+y)}{\cosh kh}\sin\left[k(x\cos\beta + z\sin\beta) - \omega t\right] \qquad (2.36)$$

and:

$$\eta^2 = \frac{g^2\eta^2{}_a}{4}\frac{\cosh^2 k(h+y)}{\cosh kh}\sin^2\left[k(x\cos\beta + z\sin\beta) - \omega t\right] \qquad (2.37)$$

Performing the time averaging and integration of the second term of equation (2.29), the following result is obtained:

$$\frac{\rho g L\eta_a\cosh^2 k(h+y)}{16\cosh^2 kh}\left(1 - \frac{1}{2}\sin k(x\cos\beta + z\sin\beta)\right) \qquad (2.38)$$

2.6 Numerical Example

The wave drift force has been calculated using the method described in the previous sections. The numerical scheme has been applied on a medium size tabular iceberg with overall dimensions of 90 x 90 x 28 meters and which has an approximate mass of 200,000 tonnes. This size of iceberg has been chosen because it approximately represents the average sizes of medium icebergs which may be encountered in the Labrador Sea and the Grand Bank area. The surface of the underwater portion of the iceberg was divided into 48 elements for the singularity distribution to obtain the converged numerical solution.

The wave drift force has been calculated in the form of a nondimensional factor, namely the wave drift force coefficient C_{wd} and it can be written as:

$$C_{wd} = F_{wd} / (1/2 \rho g L \eta_a^2) \qquad (2.39)$$

Where:

F_{wd} = wave drift force.

η_a = wave amplitude.

Wave drift forces have been calculated for waves of different periods T, with consideration given to three periods, namely $T = 12$ seconds, $T = 14$ seconds, and $T = 16$ seconds. Also wave drift force coefficients have been computed for waters with different depths h: 100 meters, 150 meters, and greater than 150 meters. Results of these calculations are shown in Figures 4 and 5. The wave drift force depends on both wave period and water depth up to a depth of 150 meters, in this particular case. It was also found that the wave drift force increases with the increase of the wave amplitude.

CHAPTER III

EQUATION OF MOTION — ICEBERG DRIFTING

In order to predict iceberg movement under the effect of various environmental forces, the equation of motion of the iceberg has to be developed and then solved. Many attempts have been made, in the past, to determine the trajectory of icebergs, such as Sodhi and Dempster [1], Napoleoni [2], Mountain [3], Sodhi and El-Tahan [4]. In these works mainly wind and current forces were considered. The wave drift action on icebergs had always been ignored in the past. In this study the wave drift force as well as other environmental forces such as current, geostrophic current, wind and Coriolis effect have been considered in formulating a more accurate equation of motion of icebergs.

3.1 Equation of Motion for Icebergs

Icebergs are subjected to a wide variety of environmental forces which vary in magnitude and relative direction, and also which depend on the location of icebergs on the earth's surface. The drift of any iceberg occurs due to the interaction between these forces and the iceberg itself. This interaction, in turn, depends on iceberg size and geometrical shape.

The interaction between iceberg and environmental forces and the resulting drift can be represented as the following differential equation of motion:

$$\left[m + \delta m\right] \ddot{\vec{\xi}} + \left[C\right] \dot{\vec{\xi}} + \left[K\right] \vec{\xi} = \vec{F}_e \tag{3.1}$$

Where:

$[m]$ = Mass matrix

$[\delta m]$ = Added mass matrix

$[C]$ = Wave damping coefficients matrix

$[K]$ = Hydrostatic restoring coefficients matrix

$\vec{F}_e$ = Environmental forces vector

$\vec{\xi}$ = Displacement vector

$\dot{\vec{\xi}}$ = Velocity vector

$\ddot{\vec{\xi}}$ = Acceleration vector.

The oscillatory motion of the iceberg is assumed to be sufficiently "small" then the added mass due to local wave disturbance and the damping effect due to radiated waves are neglected. However, the added mass of the iceberg due to the translatory acceleration is taken into consideration. Equation (3.1) can further be simplified as:

$$\left[m + \delta m\right] \ddot{\vec{\xi}} + \left[K\right] \vec{\xi} = \vec{F}_e \tag{3.2}$$

The translatory motion of an iceberg is only limited in the horizontal x - z plane, and the hydrostatic restoring forces can be negligable, equation (3.2) is then reduced to:

$$\left[m + \delta m\right] \ddot{\vec{\xi}} = \vec{F}_e \tag{3.3}$$

Equation (3.3) can be written as a set of two component differential equations in x and z directions:

$$\begin{aligned} (m + m_{11})\ \ddot{x} &= \Sigma F_x \\ (m + m_{33})\ \ddot{z} &= \Sigma F_z \end{aligned} \tag{3.4}$$

Where:

m = Iceberg mass

m_{11} = Added mass of iceberg in x direction

m_{33} = Added mass of iceberg in z direction

ΣF_x = Environmental forces acting in the x direction.

ΣF_z = Environmental forces acting in the z direction.

The environmental forces acting on the iceberg are to be taken as, wave drift force, air drag, current force, force due to gestrophic current and Coriolis force. Equation (3.4) can be written more explicitly in the component form:

$$(m + m_{11})\frac{du}{dt} = (F_{wd})_x + 1/2\ C_a \rho_a A_a V_a^2 \sin\theta + m_q \gamma\ (w - w_{cq})$$

$$+ 1/2\ C_w \rho \cdot \sum_{q=1}^{n} A_{wq} \cdot (u_{cq} - u) \cdot |\vec{V}_{cq} - \vec{V}|$$

$$(m + m_{33})\frac{dw}{dt} = (F_{wd})_z + 1/2\ C_a\rho_a A_a V_a^2 \cos\theta + m_q\gamma\ (u - u_{cq})$$

$$+ 1/2\ C_w\rho\ \sum_{q=1}^{n} A_{wq} \cdot (w_{cq} - w) \cdot |\vec{V}_{cq} - \vec{V}| \quad (3.5)$$

Where:

$\vec{V}$ = (u,w), ~~iceberg~~ iceberg velocity.

$\vec{V}_a$ = (u_a, w_a), wind velocity.

$\vec{V}_{cq}$ = (u_{cq}, w_{cq}), water current velocity at qth layer of iceberg underwater, including both Ekman and geostrophic currents.

m_q = Mass of displaced water by iceberg in qth layer.

C_a = Air drag coefficient.

ρ_a = Air density.

C_w = Water drag coefficient.

ρ = Water density.

A_a = Area of iceberg profile above water, perpendicular to wind direction.

A_{wq} = Area of iceberg profile of qth layer of underwater portion, perpendicular to current direction.

γ = $2\Omega\sin\psi$, Coriolis parameter.

Ω = Angular velocity of earth.

ψ = Iceberg latitude.

θ = Wind direction.

From Reference [4], coefficients C_a and C_w are taken as 1.5 and 1 respectively; and the added mass of the iceberg due to translatory acceleration is assumed to be one-half of the iceberg mass for x and z directions, $m_{11} = m_{33} = \frac{1}{2}$ m. The underwater projected area A_a is 1800 m^2.

3.2 Solution of the Equation of Motion - Iceberg Trajectory

The iceberg trajectory will be predicted from the solution of the differential equation governing its translatory motion, namely, the following initial value problem:

$$\frac{dx}{dt} = u$$

$$\frac{dz}{dt} = w$$

$$\frac{du}{dt} = \frac{1}{(m + m_{11})} \Sigma F_x$$

$$\frac{dw}{dt} = \frac{1}{(m + m_{33})} \Sigma F_z \qquad (3.6)$$

The initial conditions are determined as follows:

- The initial location of iceberg (x_o, z_o) is where the iceberg was when first sighted, in nautical miles, from the reference sighting point.
- The initial velocity of iceberg (u_o, w_o) is its velocity when first sighted, in x and z directions.

The numerical method used to solve the equations of motion in this study is the time step integration technique. The equations are stepped forward in time to yield predicted positions. The values at time $t + \Delta t$ are obtained by the first order Taylor series expansion.

Velocities of the iceberg are obtained from the following relations:

$$u(t_1 + \Delta t) = u(t_1) + \Delta t \cdot \dot{u}(t_1)$$

$$w(t_1 + \Delta t) = w(t_1) + \Delta t \cdot \dot{w}(t_1) \qquad (3.7)$$

Where:

Δt = Time step.

The location of the iceberg $x(t)$ and $z(t)$ are obtained from the following relations in conjunction with equation (3.7).

$$x(t_1 + \Delta t) = x(t_1) + \Delta t \cdot u(t_1)$$

$$z(t_1 + \Delta t) = z(t_1) + \Delta t \cdot w(t_1) \qquad (3.8)$$

The accelerations $\dot{u}$, $\dot{w}$ and velocities u, w of an iceberg are assumed to be varying slowly with time, this is due to the large mass and inertia of an iceberg compared to the relatively small environmental forces acting on it. The method of time step integration gives sufficiently accurate solutions, and requires less computing time compared with other methods. However, the choice of initial values of accelerations, velocities and the time step size will effect the computed results.

3.3 Two Examples from Field Data

The mathematical drift model developed in the previous sections has been tested and verified by comparing the trajectories of two icebergs obtained from the field measurements. The data of measured trajectories were taken from the field observations in the Labrador Sea during the offshore drilling season of 1974 [7].

Three sets of data should be available to check the mathematical drift model, namely, the iceberg size and geometry, environmental data, and the observed trajectory. These data were arranged and prepared in a format suitable for computer applications.

(a) Iceberg Size and Geometry

The two icebergs used in this study were iceberg number G181 which was first sighted at 1300 hours on the 3rd of September, 1974, and iceberg number G183 which was first sighted at 800 hours on the 4th of September, 1974. The two icebergs had a mass of approximately 200,000 tonnes with a tabular shape.

(b) Iceberg Trajectory

For each iceberg, the trajectory was established from the field measurements of distance and bearing by radar with respect to the observation station. The observation station was located on the bridge of the drillship Pelican and consisted of two identical port and starboard radar systems with the following specifications:

Manufacturer	Kelvin Hughes
Wave Length	2cm x band
Display units	Model 19/12 gyro-stabilized with variable range cursor.
Antenna length	2.3 meter
Transmitted power	25 KW

The efficiency of the radar for iceberg detection was established from previous observations (1973), and is summarized in Table 2, which gives the relation between maximum detection range "R" of bergs and the percentage of berg detection. As shown in Table 2, half of the bergs were not seen on radar until they were about 16 miles away and, 20 percent were not detected until they were 8 miles away. Those not detected until they were within range of 4 to 5 miles and less were usually bergy bits.

Observations were taken every hour and recorded in the iceberg log from the moment the iceberg was first sighted until it was safely away from the drill ship. The table of location and bearings of the iceberg was used as input file, and the observed trajectory was plotted using the computer plotting routine. Iceberg logs for icebergs G181 and G183 taken on the ship are shown in Figures 7 to 10, respectively.

(c) Environmental Data

Environmental data were obtained from the daily observation log on board the drillship Pelican. The observation log provides all environmental data which have been measured and compiled at a particular location. These data consist of:

1. Wind speed and mean direction:

All wind speed and direction measurements were made on drillship Pelican every hour with ship's anemometer. Dial readouts of wind speed and direction (relative to ship's heading) were recorded. True wind direction was taken by adding the dial reading and the ship's heading from the gyro-compass. All wind measurements were taken as mean values of 1-2 minute.

2. Wave height and direction:

All wave measurements were taken by using a data well waverider buoy and associated equipment. Moored about 0.6 miles from the ship, the buoy sensed acceleration which were then double integrated to convert them to wave heights. It transmitted wave height continually to a receiver mounted on the ship. The recorder was programmed to switch on for sampling periods of 20 minutes in 3 hours. Continuous records were possible by overriding the timer. From the wave recorder wave heights and wave directions are filed in the observation logs as shown in Tables 3 to 8.

3. Current speed and direction:

Current measurements were obtained every hour from three separate direct-reading current meters on the Pelican. The first one was the ship's own electromagnetic current meter, fixed beneath the hull near the moon pool. The readout from this meter was with dial indicator on the bridge. The other two meters of type BFM008 and BFM008, ME.2 were suspended from the bow of the ship at depths of 15 meters and 50 meters, respectively. The read-out units for these units were mounted on ship's bridge. The meters had a speed accuracy of the range of 2 percent and direction accuracy of the range of 10^{o}.

The daily observation logs for icebergs G181 and G183 are shown from Tables 3 to 8. The observed trajectories of these two icebergs are shown from Figures 6 to 9. Computed trajectories with the wave effect plotted together with the respective observed trajectories are presented in Figures 10 to 13. Computation for iceberg G181 started at 1700 hours, September 3, 1974, and ended at 1900 hours, September 5, 1974. Computation for iceberg G183 started at 1100 hours, September 9, 1974, and ended at 0500 hours, September 11, 1974.

CHAPTER IV

CONCLUDING REMARKS

The wave drift force acting on icebergs has been presented and calculated in this thesis. The calculation of the wave drift force is based on a three-dimensional singularity distribution method. It was found that the magnitude of the wave drift force is of the same order as other environmental forces such as current, wind or Coriolis forces. It was also found that the wave drift force depends on the size of the iceberg and in particular the size of its waterplane. The wave characteristics affect the magnitude of drift force which is proportional with the square of wave amplitude and decreases with the increase of wave period. In addition the wave drift force was found to be affected by the change in water depth.

The iceberg drift model used in this study is based on the numerical solution of the differential equations of motion. The time step integration has been applied to the numerical scheme. The accuracy of the results depend on the input parameters as well as the numerical method itself. The input parameters of an iceberg are its mass, surface area, and location based on field observations and can have the measuring errors of the order up to 40% in some cases.

The accuracy of environmental forces depend on quality of the measuring and recording instruments. These instruments have inherited errors as mentioned in Chapter 3. Parameters such as water drag, wind drag and added mass coefficients are assumed to have values taken from existing literatures, but not necessarily the most reliable values. The size of time step has been taken as one hour because most environmental data as well as ranges and bearings of icebergs were measured and recorded in the interval of one hour. It is assumed that the iceberg has a steady motion within this time interval, this is due to the large mass and inertia of an iceberg compared to the relatively small environmental forces acting on it. Decreasing the size of the time step may improve the accuracy of the results, but this requires data to be recorded in shorter time intervals.

It is expected that there will be deviations between observed trajectories and numerically calculated trajectories of icebergs due to different types of errors and methods of approximation. In particular, the selection of initial conditions of the iceberg motion and location will affect the computed trajectory. From Figures 10 to 13 it is interesting to observe that including the added mass in computing iceberg trajectories may not improve the predicted drift pattern significantly.

The results obtained from this study have shown that it is important to include the effect of wave action in predicting the iceberg drift pattern. The improvement of accuracy in predicting the drift pattern will enable the operator of any offshore installation to make the right decision, at the right time, regarding evacuation or suspension of drilling activities when an iceberg is approaching the site.

In this study, the wave drift force is based on the regular wave analysis, and only applied to the icebergs of tabular shape. Future research is needed to investigate the drifting behavior of icebergs of other shapes and sizes with the irregular wave theory.

Finally, the results obtained in this thesis have proved that the wave drift force acting on icebergs of medium or small size is significant. It is highly recommended that for any future mathematical modelling of iceberg drift the wave drift effect should never be overlooked.

REFERENCES

1. Sodhi, D.S., and Dempster, R.T., "Motion of Icebergs Due to Changes in Water Currents", IEEE, Oceans 75, 1975, pp. 348 - 398.

2. Napoleni, J.C., "The Dynamics of Iceberg Drift", M.Sc. Thesis, Department of Geophysics and Astronomy, University of British Columbia, Canada, 1979.

3. Mountain, D.C., "On Predicting Iceberg Drift", Iceberg Dynamic Conference, St. John's, Newfoundland, Canada, June 1979, and Cold Region Science and Technology, Vol. 1, 1980, pp. 273 - 282.

4. Sodhi, D.S., and El-Tahan, M., "Prediction of an Iceberg Drift Trajectory During a Storm", Annals of Glaciology, Vol. 1, 1980, pp. 77 - 82.

5. Faltinson, O.M., and Micholson, F., "Motions of Large Structures in Waves at Zero Froude Number", Proceedings of International Symposium on the Dynamics of Marine Vehicles and Structures in Waves, London, England, 1974, pp. 91 - 106.

6. Pinkster, J.A., and Van Oortmersson, G., "Computation of the First and Second Order Wave Forces on Bodies Oscillating in Regular Waves", Proceedings of 2nd International Conference on Numerical Ship Hydrodynamics, University of California, Berkely, U.S.A., 1977, pp. 136 - 156.

7. "Offshore Labrador Environmental Conditions, Summer of 1974", Published by Marine Environmental Service Limited, Calgary, Canada.

8. Wehausen, J.V., and Laitone, E.E., "Surface Waves", Handbuch der Physik, 9. 1969, Springer-Verlag, Berlin 1969.

9. Zienkiewicz, O.C., Lewis, R.W., and Stagg, K.G., (Eds.), "Numerical Methods in Offshore Engineering", John Wiley, New York, 1978.

Force Components	Force $\times 10^4$N	Condition	Force $\times 10^4$N	Condition	Force $\times 10^4$N	Condition
Water Drag	5.35	Relative Vel. = 0.2 m/sec.	15.12	Relative Vel. = 0.4 m/sec.	34.02	Relative Vel. = 0.6 m/sec.
Wind Drag	1.95	Wind Speed = 20 knots	7.8	Wind Speed = 40 knots	17.55	Wind Speed = 60 knots
Coriolis Effect	0.76	Latitude = 55° Rel. Vel = 0.2 m/sec.	1.52	Latitude = 55° Rel. Vel = 0.4 m/sec.	2.27	Latitude = 55° Rel. Vel = 0.6 m/sec.
Geostropic Effect	4.0	Acceleration = 2×10^{-5} m/sec^2	8.0	Acceleration = 4×10^{-5} m/sec^2	12.0	Acceleration = 6×10^{-5} m/sec^2
Wave Drift Effect	8.11	Wave Amp = 0.5m Wave Period = 12 sec.	32.45	Wave Amp = 1.0m Wave Period = 12 sec.	73.00	Wave Amp = 1.5m Wave Period = 12 sec.

Table 1 Comparison Between the Magnitude of a Variety of Environmental Forces Acting on a 200,000 Tonne Tabular Iceberg

Maximum Detection Range "R" of Bergs and Bergy Bits	Percent of Bergs Detected at Ranges Greater than "R"
N. Miles	%
0.0	100
2.0	99
4.0	96
6.0	88
8.0	82
10.0	78
12.0	72
16.0	52
20.0	34
24.0	7

Table 2. Relation Between Maximum Detection Range "R" of Bergs and The Percentage of Berg Detection (Reference 8)

NAME OF VESSEL: PELICAN			DAILY OBSERVATION LOG
POSITION	Latitude: 54°54′ N	Date: 3Sept 1974	
	Longitude: 55°52′ W	Time Zone: GMT-3HR	

Time (Local)	WINDS			WAVES						CURRENTS			
	Mean Hourly Speed	Max. Gust and Meas. Duration	Mean Wind Dir.	Signif. Wave Height	Max. Height (3 hrs.)	Mean Zero Crossing Period	Swell Height	Swell Period	Wave Dir.	15 m		50 m	
										Speed (kts)	Dir. (Towards)	Speed (kts)	Dir. (Towards)
0100	24		275							.34	090	.16	210
0200	24		270							.26	110	.12	200
0300	25		270	3.1	5.9	4.9				.38	150	.13	180
0400	33		275							.60	180	.14	200
0500	29		275							1.04	240	.18	220
0600	25		275	3.8	7.4	5.7		wave	270°	.88	210	.17	220
0700	29		275							0.96	250	0.13	190
0800	25		275							0.85	260	0.14	140
0900	24		280	3.8	7.2	5.1		wave	290°	0.62	270	0.17	110
1000	25		275							0.58	230	0.10	140
1100	29		280							0.27	070	0.13	160
1200	29		285	3.6	6.8	5.3		wave	290°	0.05	040	0.12	120
1300	25		290							.19	090	.17	140
1400	24		290							.21	120	.14	150
1500	26		280	4.1	7.8	4.6				.22	130	.10	180
1600	27		280							.16	130	.07	160
1700	27		290							.56	130	.11	130
1800	30		290	3.4	6.5	5.2		wave	290°	.31	140	.03	100
1900	25		290							0.31	140	0.11	140
2000	24		290							0.58	180	0.07	160
2100	25		300	2.9	5.5	5.0		wave	290°	0.55	140	0.12	050
2200	24		300							0.39	150	0.07	120
2300	22		295							0.19	150	0.14	090
2400	21		295	3.2	5.0	5.0		wave	290°	0.19	100	0.13	100

Table 3. Daily Observations Log Iceberg G181 (Reference 8)

NAME OF VESSEL: PELICAN		
POSITION	Latitude: 54°54′ N	Date: 4Sept 1974
	Longitude: 55°52′ W	Time Zone: GMT-3

DAILY
OBSERVATION
LOG

Time (Local)	WINDS			WAVES						CURRENTS			
	Mean Hourly Speed	Max. Gust and Meas. Duration	Mean Wind Dir.	Signif. Wave Height	Max. Height (3 hrs.)	Mean Zero Crossing Period	Swell Height	Swell Period	Wave Dir.	15 m Speed (kts)	15 m Dir. (Towards)	50 m Speed (kts)	50 m Dir. (Towards)
0100	22		290							.05	160	.15	110
0200	21		295							.08	100	.12	090
0300	21		300	2.9	5.5	4.8				.08	150	.18	120
0400	19		300							.09	110	.14	130
0500	18		300							.10	100	.09	160
0600	15		290	2.9	5.3	5.0				.08	070	.14	190
0700	13		285							0.05	070	0.12	240
0800	15		295							0.10	110	0.14	120
0900	14		290	2.6	4.9	5.1		wave	310°	0.19	090	0.11	050
1000	13		300							0.11	130	0.10	130
1100	11		340					wave	330°	0.28	120	0.13	070
1200	13		295	2.5	4.8	4.9		wave	300°	0.22	130	0.12	080
1300	10		300							.11	140	.09	070
1400	08		290							.08	140	.10	070
1500	08		290	2.3	4.4	6.5				.05	160	.12	080
1600	06		295							.02	120	.13	080
1700	04		330							.27	360	.12	100
1800	02		010	2.2	4.2	7.4	2.0	7	350°	.32	040	.08	100
1900		CALM								0.17	060	0.10	280
2000		CALM								0.32	050	0.10	070
2100		CALM		1.7	3.3	6.1			340°	0.30	050	0.10	140
2200	7		180							0.53	060	0.07	010
2300	5		175							0.48	100	0.06	030
2400	4		170	1.8	3.5	6.3			330°	0.49	100	0.10	350

Table 4. Daily Observations Log Iceberg G181 (continued)

NAME OF VESSEL: PELICAN		
POSITION	Latitude: 54°54′ N	Date: 5Sept 1974
	Longitude: 55°52′ W	Time Zone: GMT-3

DAILY OBSERVATION LOG

Time (Local)	WINDS			WAVES						CURRENTS			
	Mean Hourly Speed	Max. Gust and Meas. Duration	Mean Wind Dir.	Signif. Wave Height	Max. Height (3 hrs.)	Mean Zero Crossing Period	Swell Height	Swell Period	Wave Dir.	15 m		50 m	
										Speed (kts)	Dir. (Towards)	Speed (kts)	Dir. (Towards)
0100	01		180							.32	100	.11	050
0200	04		140							.16	110	.10	050
0300	06		130	2.0	3.8	6.4	2.0	6.4	020	.07	120	.06	070
0400	07		140							.06	120	.06	020
0500	07		120							.05	030	.06	050
0600	06		130	1.9	3.6	7.1	1.9	7.1	020	.05	040	.13	020
0700	07		120							0.02	090	0.13	280
0800	8		115							0.05	340	0.09	000
0900	8		120	1.6	3.0	6.7			010	0.22	060	0.10	020
1000	7		130							0.25	050	0.11	060
1100	6		125							0.39	060	0.12	060
1200		CALM		3.0	5.8	7.2	2.0	7.21	015	0.36	070	0.10	070
1300	2		130							.52	080	.11	130
1400	2		135							.38	080	.07	120
1500	3		190	1.7	3.3	6.6	1.7	6.6	020	.27	110	.11	100
1600	4		180							.26	110	.09	140
1700	6		180							.13	110	.09	290
1800	5		170	1.5	2.8	7.2			030	.09	130	.06	300
1900	8		170							0.09	130	0.12	300
2000	6		170							.20	010	.06	350
2100	15		180	1.5	2.8	6.7				.05	140	.11	350
2200	13		180							.06	100	.05	010
2300	17		190							.19	100	.06	030
2400	17		230	1.8	3.5	5.3				.13	100	.08	120

Table 5. Daily Observations Log Iceberg G181 (continued)

NAME OF VESSEL: PELICAN			DAILY OBSERVATION LOG
POSITION	Latitude: 54°54′ N	Date: 9Sept 1974	
	Longitude: 55°52′ W	Time Zone: GMT-3	

Time (Local)	WINDS			WAVES						CURRENTS			
	Mean Hourly Speed	Max. Gust and Meas. Duration	Mean Wind Dir.	Signif. Wave Height	Max. Height (3 hrs.)	Mean Zero Crossing Period	Swell Height	Swell Period	Wave Dir.	15 m		50 m	
										Speed (kts)	Dir. (Towards)	Speed (kts)	Dir. (Towards)
0100	23		165							.30	080	.29	310
0200	25		175							.34	090	.29	320
0300	23		170	2.6	4.9	4.5				.11	070	.26	340
0400	21		175							.26	070	.26	350
0500	23		180							.29	080	.32	360
0600	21		180	2.4	4.6	4.5			180	.16	070	.16	340
0700	21		190							.26	070	.23	310
0800	20		185							.37	090	.23	310
0900	24		195	2.5	4.8	4.5				.24	140	.20	320
1000	22		200							.14	140	.10	320
1100	18		205							.06	120	.40	280
1200	18		220	2.0	3.8	4.3				.37	110	.52	300
1300	13		225							.43	050	.21	300
1400	15		250							.51	030	.16	240
1500	15		255	1.6	3.0	4.4	1.5	4.5	160	.67	030	.25	310
1600	14		335							.39	110	.20	330
1700	12		330							.39	010	.20	340
1800	5		325	1.1	2.1	4.7				.37	310	.32	330
1900	6		340							.46	330	.33	330
2000	6		345							.45	330	.34	320
2100	5		325	1.3	2.5	4.4				.54	340	.35	340
2200	2		300							.35	360	.09	340
2300	12		240							.11	120	.14	270
2400	3		180	1.2	2.3	6.0				.51	170	.15	300

Table 6. Daily Observations Log Iceberg G183 (Reference 8)

NAME OF VESSEL: PELICAN		
POSITION	Latitude: 54°54′ N	Date: 10Sept 1974
	Longitude: 55°52′ W	Time Zone: GMT-3

DAILY
OBSERVATION
LOG

Time (Local)	WINDS			WAVES						CURRENTS			
	Mean Hourly Speed	Max. Gust and Meas. Duration	Mean Wind Dir.	Signif. Wave Height	Max. Height (3 hrs.)	Mean Zero Crossing Period	Swell Height	Swell Period	Wave Dir.	15 m		50 m	
										Speed (kts)	Dir. (Towards)	Speed (kts)	Dir. (Towards)
0100	4		180							.24	040	.15	250
0200	8		190							.38	060	.08	310
0300	10		200	0.8	1.5	6.9				.17	060	.14	270
0400	14		220							.22	040	.25	330
0500	15		250							.03	040	.02	050
0600	24		300	1.1	2.1	4.5	0.5	7	260	.07	040	.20	210
0700	14		290							.16	130	.27	360
0800	20		290							.33	100	.27	360
0900	22		290	1.8	3.5	4.0	–		290	.24	130	.13	360
1000	24		295							.35	150	.12	340
1100	20		270							.11	070	.16	010
1200	20		270	2.0	5.1	3.8				.16	130	.31	280
1300	14		260							.13	100	.35	350
1400	13		265							.16	070	expecting	
1500	17		270	2.2	4.2	4.8				.07	100	storm	
1600	12		255							.09	070	–	–
1700	10		235							.20	050	–	–
1800	23		270	2.5	4.8	5.1		7	310	.45	070	–	–
1900	13		240					mostly		.39	070	–	–
2000	12		220					swell		.50	070	–	–
2100	15		225	2.6	4.9	4.4				.56	090	–	–
2200	19		245							.45	080	–	–
2300	24		250							.31	090	–	–
2400	21	-	260	2.7	5.1	4.2				.25	120	–	–

Table 7. Daily Observations Log Iceberg G183 (continued)

NAME OF VESSEL: PELICAN		
POSITION	Latitude: 54°54′ N	Date: 11Sept 1974
	Longitude: 55°52′ W	Time Zone: GMT-3hr

DAILY OBSERVATION LOG

Time (Local)	WINDS: Mean Hourly Speed	WINDS: Max. Gust and Meas. Duration	WINDS: Mean Wind Dir.	WAVES: Signif. Wave Height	WAVES: Max. Height (3 hrs.)	WAVES: Mean Zero Crossing Period	WAVES: Swell Height	WAVES: Swell Period	WAVES: Wave Dir.	CURRENTS 15 m: Speed (kts)	CURRENTS 15 m: Dir. (Towards)	CURRENTS 50 m: Speed (kts)	CURRENTS 50 m: Dir. (Towards)
0100	25	29.5	250							.23	120		
0200	25		250							.20	160		
0300	24		250	3.5	6.7	4.5		wave	250	.03	120		
0400	25		250							.18	170		
0500	26		250							.12	100		
0600	26		240	2.3	5.3	5.0				.11	100		
0700	26		235							.12	100		
0800	25		240							.42	060		
0900	25		240	3.4	6.5	5.6				.36	010		
1000	22		240										
1100	26		240										
1200	23		245	3.7	7.0	4.9			290				
1300	21		250										
1400	19		265										
1500	22		265	4.0	7.5	5.1			300				
1600	19		275										
1700	13		255										
1800	18		295	3.1	5.9	5.0			295				
1900	27		295										
2000	14		265										
2100	14		270	3.1	5.9	5.5			290				
2200	13		260										
2300	12		240										
2400	10		240	2.3	4.4	5.7							

Table 8. Daily Observations Log Iceberg G183 (continued)

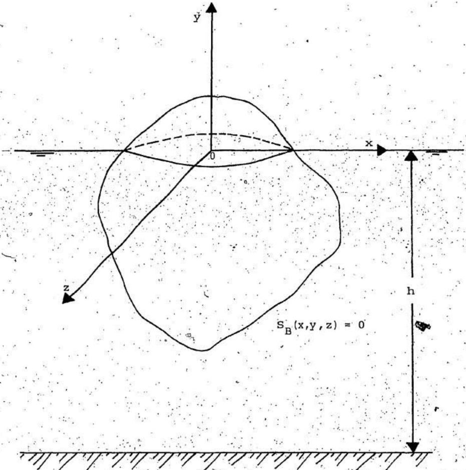

Figure 1. Co-ordinate System of a Floating Iceberg.

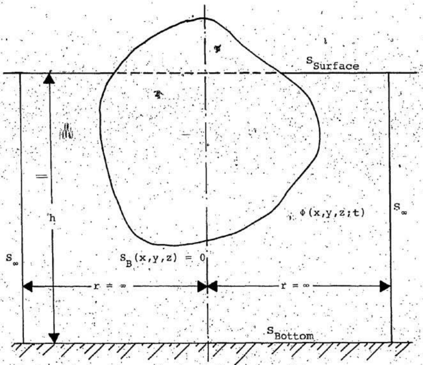

Figure 2. Geometrical Boundaries of the Hydrodynamic Boundary Value Problem

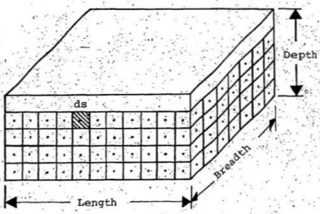

Figure 3. Distribution of Elements on the Submerged Surface of a Floating Body

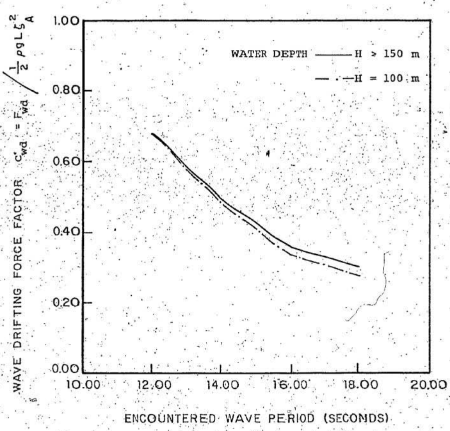

Figure 4. WAVE DRIFTING FORCE FACTOR FOR A 200,000 TONNES TABULAR ICEBERG RELATED TO ENCOUNTERED WAVE PERIOD.

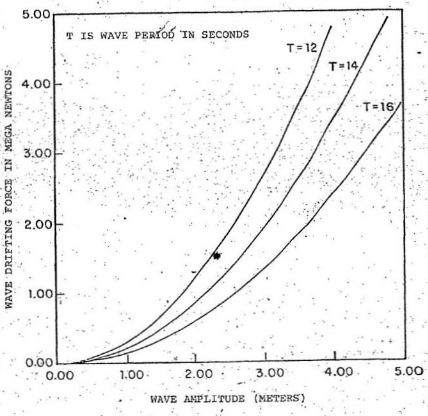

Figure 5. WAVE DRIFTING FORCE ACTING ON A 200,000 TONNES TABULAR ICEBERG RELATED TO WAVE AMPLITUDE.

ICEBERG LOG: PELICAN IDENTIFICATION No. G181

DATE:TIME 3Sept 74	Range Nautical Miles	Bearing Relative True N.
1300	16.8	320
1400	16.0	320
1500	15.0	320
1600	13.7	320
1700	12.8	321
1800	11.8	321
1900	10.8	322.5
2000	9.6	322.5
2030	8.8	323
2100	8.6	323.5
2130	8.0	323.5
2200	7.8	323
2230	7.2	324
2300	7.1	324.5
2330	6.8	326.5
2400	6.6	328.5
4Sept		
0100	6.1	334
0200	5.8	342
0300	5.5	351
0400	5.6	357
0500	5.8	004
0600	6.1	013
0700	6.5	018.5
0800	6.5	025.5
0900	6.7	033
1000	6.7	039
1100	6.8	044.5
1200	6.9	049.5
1300	7.2	056
1400	7.3	061
1500	7.3	065
1600	7.6	066
1700	7.7	066
1800	7.8	066
1900	7.6	066.5
2000	7.8	066
2100	8.2	067.5
2200	8.3	069.5
2300	8.5	071.5
2400	8.7	73.7

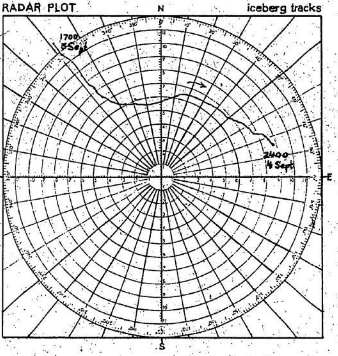

NOTES:

max. wt. 300,000 tons
prob. wt. 200,000 tons

Figure 6. Iceberg Log of G181 (Reference 8)

ICEBERG LOG: PELICAN IDENTIFICATION No. G181

DATE:TIME 3Sept 74	Range Nautical Miles	Bearing Relative True N.
0100	9.8	077
0200	9.6	078
0300	9.6	081
0400	9.6	083
0500	9.6	083
0630	9.6	084
0700	9.6	084
0800	9.8	084.5
0900	9.8	085
1000	10.0	086.5
1100	10.4	087.5
1200	10.6	089
1300	11.1	091
1400	11,3	093
1530	11.8	094
1630	11.9	095
1730	12.3	096
1900	12.6	098
2000	12.9	100
2100	13.0	101
2200	13.2	101
2300	13.5	103
2400	14.0	103
6Sept		
0100	14.7	102
0300	15.3	102

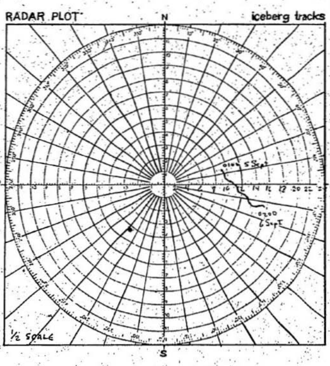

NOTES:

Figure 7. Iceberg Log of G181 (continued)

ICEBERG LOG: PELICAN

IDENTIFICATION No. G183

DATE:TIME 9Sept 74	Range Nautical Miles	Bearing Relative True N.
1100	4.00	316
1200	4.6	316
1300	5.2	314
1400	5.6	315
1500	5.7	317
1600	5.6	319.5
1700	5.6	319.5
1800	6.1	319
1900	6.3	318
2000	6.6	317
2200	7.1	313
2300	7.9	314
2400	8.1	315
10Sept		
0100	8.2	314
0200	8.3	314
0300	8.9	316
0400	8.8	317
0500	8.9	319
0600	8.6	320
0700	8.6	320
0800	8.5	320
0915	8.5	319
1000	8.3	317
1100	8.4	318
1200	8.1	317
1300	8.0	316
1400	8.3	316
1500	8.1	317.5
1600	8.2	317.5
1700	8.6	319
1800	8.4	322.5
1900	8.1	323.5
2000	8.1	326
2100	8.1	328
2200	8.0	329
2300	7.7	330
11Sept		
0030	7.4	334
0130	7.1	338
0310	7.0	348
0500	7.2	358

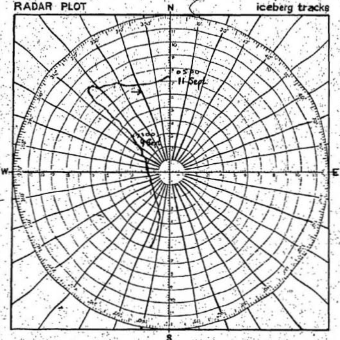

NOTES:

Figure 8. Iceberg Log of G183 (Reference 8)

ICEBERG LOG: PELICAN IDENTIFICATION No. G183

DATE:TIME 11Sept 74	Range Nautical Miles	Bearing Relative True N.
0600	7.3	005
0700	7.3	013
0800	8.0	021
0900	8.8	027
1000	8.8	032
1100	9.2	037
1200	9.5	041
1300	9.9	047
1400	10.4	050
1500	10.9	053
1600	11.2	056
1700	11.6	058.5
1800	11.9	061
1900	12.3	065
2000	12.7	069
2100	13.0	071
2200	13.3	073
2300	not	seen

RADAR PLOT iceberg tracks

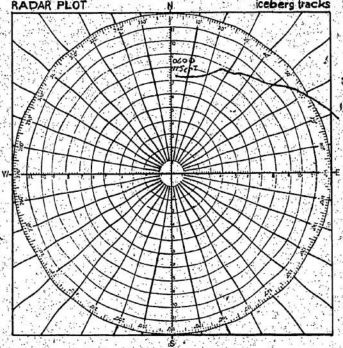

NOTES

Figure 9. Iceberg Log of G183 (continued)

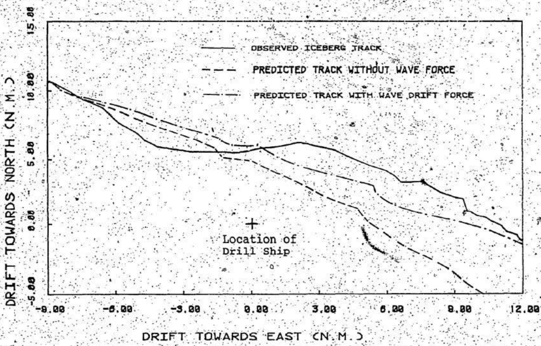

FIGURE 10. DRIFT TRAJECTORY OF ICEBERG 6181

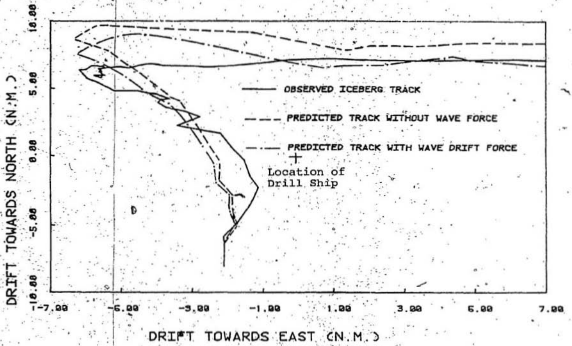

FIGURE 11. DRIFT TRAJECTORY OF ICEBERG G183

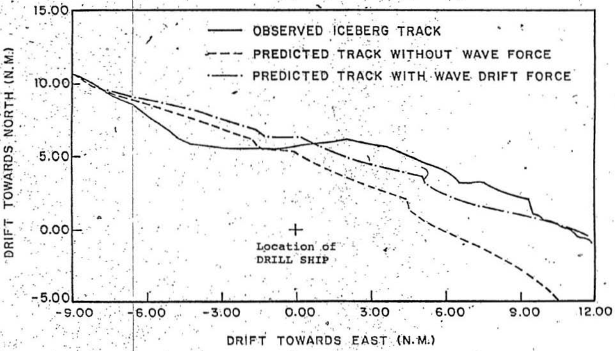

Figure 12. DRIFT TRAJECTORY OF ICEBERG G181
(Added mass of iceberg is not included in the equation of motion of the iceberg).

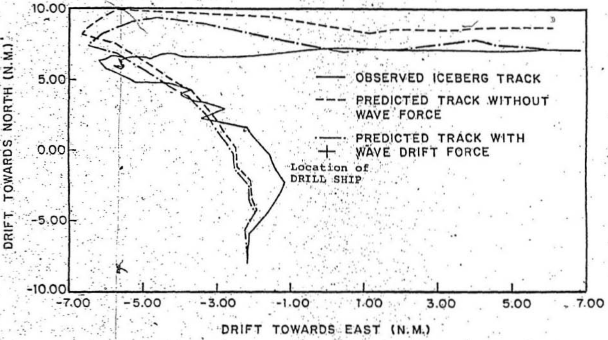

Figure 13. DRIFT TRAJECTORY OF ICEBERG G183
(Added mass of iceberg is not included in the equation of motion of the iceberg).